Proceedings of ISAP'04, Sendai, JAPAN

MUSIC LOCALIZATION OF LOW-FREQUENCY CURRENT LOOP SOURCES

K. Ishibana[1], S. Yagitani[1], M. Kawauchi[1], I. Nagano[1],
Y. Yoshimura[2], H. Hayakawa[3], K. Tsuruda[3]
[1]Graduate School of Natural Science and Technology, Kanazawa University
2–40–20 Kodatsuno, Kanazawa 920–8667, Japan
[2]Industrial Research Institute of Ishikawa, 2–1 Kuratsuki, Kanazawa 920–8203, Japan
[3]Institute of Space and Astronautical Science, Japan Aerospace Exploration Agency
3–1–1 Yoshinodai, Sagamihara 229–8510, Japan
E-mail ishibana@reg.is.t.kanazawa-u.ac.jp

1. Introduction

It is important to identify the locations of electromagnetic (EM) noise sources within the electrical and electronic equipment, for the reduction of undesired noise emissions from it. To search for the EM noise sources in the equipment under real operating conditions, usually we need to determine their locations from the EM field distributions observed around it. By observing the vector magnetic fields around the small current loop sources at low frequencies (less than tens of MHz), we have applied the MUSIC algorithm to estimate the locations and orientations of them assuming that they are point sources (magnetic dipoles) [1]. However, actual current loops existing in the equipment usually have finite sizes, for which our previous MUSIC algorithm would not be accurately applicable.

In this study, we extend the MUSIC algorithm to localize the finite-size current loop sources, by estimating their sizes in addition to their locations and orientations. We evaluate the applicability of this algorithm with simulation.

2. MUSIC localization of current loop sources

First we briefly explain the MUSIC algorithm [2][3][4] to estimate the 3-d locations and orientations of the low-frequency magnetic dipoles [1]. As shown in Fig. 1, we have N_S incoherent source magnetic dipoles at arbitrary locations $\boldsymbol{l}_{S,i}$ and orientations $\boldsymbol{d}_{S,i}$ (i=1, 2, $\cdots$, N_S). The source signals $s_i(t)$ input to the dipoles are assumed to be narrowband, and locations and orientations of the dipoles do not change during measurement. The magnetic field distribution radiated from the source dipoles is measured by N_A magnetic sensors whose locations and orientations are given by $\boldsymbol{l}_{A,j}$ and $\boldsymbol{d}_{A,j}$ (j=1, 2, $\cdots$, N_A). Here the number of sensors N_A should be larger than the number of sources N_S.

With the eigenanalysis of the covariance matrix $\boldsymbol{R}_{xx}$ calculated from the measured magnetic field vector $\boldsymbol{X}(t)$, we have $N_A - N_S$ noise eigenvalues. The noise subspace $\boldsymbol{E}_N$ spanned by the corresponding eigenvectors is orthogonal to the steering vector for true sources, $\boldsymbol{a}_i(\boldsymbol{l}_{S,i}, \boldsymbol{d}_{S,i})$, so that we can determine the source locations and orientations, by evaluating the local maxima of the MUSIC cost function P_{music}, given as,

$$P_{music}(\boldsymbol{l}, \boldsymbol{d}) = \frac{\|\boldsymbol{a}(\boldsymbol{l}, \boldsymbol{d})\|^2}{\|\boldsymbol{E}_N^H \boldsymbol{a}(\boldsymbol{l}, \boldsymbol{d})\|^2} \tag{1}$$

where ^{H} means the Hermitian conjugate. Here $\boldsymbol{l}$ and $\boldsymbol{d}$ are the parameters to be scanned during the peak search in 5-dimensional space (3 for $\boldsymbol{l}$, 2 for $\boldsymbol{d}$). Here we can reduce the number of parameters to only 3 for $\boldsymbol{l}$. First, we decompose the steering vector into the elementary steering vectors $\boldsymbol{a}_x$, $\boldsymbol{a}_y$, and $\boldsymbol{a}_z$, which respectively correspond to x, y, and z-directed source dipoles, as $\boldsymbol{a}(\boldsymbol{l}, \boldsymbol{d}) = [\boldsymbol{a}_x|\boldsymbol{a}_y|\boldsymbol{a}_z]\ \boldsymbol{d} \equiv \boldsymbol{a}_{xyz}\boldsymbol{d}$, where we have defined $\boldsymbol{a}_{xyz} \equiv [\boldsymbol{a}_x|\boldsymbol{a}_y|\boldsymbol{a}_z]$. From this, the cost

ISBN: 4-88552-206-4 C3055©IEICE

function P_{music} can be modified as the function of only the location $\boldsymbol{l}$, as

$$P_{music}(\boldsymbol{l}, \boldsymbol{d}) = P_{music}(\boldsymbol{l}) = \frac{\boldsymbol{e}_{min}^H \boldsymbol{a}_{xyz}^H \boldsymbol{a}_{xyz} \boldsymbol{e}_{min}}{\lambda_{min}(\boldsymbol{a}_{xyz}^H \boldsymbol{E}_N \boldsymbol{E}_N^H \boldsymbol{a}_{xyz})} \tag{2}$$

where $\lambda_{min}()$ means to take the minimum eigenvalue of the matrix in the parenthesis. The modified cost function $P_{music}(\boldsymbol{l})$ takes maximum at each of true source dipole locations, where the eigenvector $\boldsymbol{e}_{min}$ corresponding to the minimum eigenvalue represents the orientations of each dipole.

When the source current loops have finite sizes, their steering vectors become different from those of point dipoles. In order to know the sizes as well as locations and orientations of the loops with the MUSIC algorithm, we need to scan the additional "loop size" space, with changing the steering vectors. This would increase, however, the computation burden of P_{music} drastically. Here, first we try to estimate the locations and orientations of the finite-size current loop sources with the point dipole model. Such estimated locations and orientations would not exactly indicate the true values, so that by changing the size of the current loops, we re-scan P_{music} in the location space limited to the vicinity of those estimated with the point dipole model. Here we tentatively fix their orientations as estimated by the dipole model, because for the finite-size current loops we cannot decompose their steering vectors to estimate their orientations as in (2).

3. Simulation

As an example of the simulation model of the MUSIC localization of the current loop sources. The MUSIC scan is done over the 3 m×3 m×3 m volume, with the resolution of 10 cm, and the number of snapshots is 2000.

3.1 Magnetic dipole sources

We have two incoherent magnetic dipole sources, #1 and #2, with the locations and orientations as the "True" values in Table 1. We put three triaxial search coil sensors at the locations (x, y, z) = (0, 0, 0), (1, 0, 0), (2, 0, 0) [m], at each of which the sensor measures the x-, y-, and z-components of the magnetic field. The frequencies of the dipole sources #1 and #2 are 10 kHz and 10.5 kHz and the their signal-to-noise ratio (SNR) are 38 dB and 47 dB, respectively. Here we define the SNR of the received signals as the ratio of each of the signal eigenvalues to the maximum of the noise eigenvalues of the covariance matrix of the sensor output. Fig. 2 (a) and (b) show the P_{music} distributions over two $x-y$ (horizontal) planes at $z = 0.0$ m and $z = -0.4$ m, for the sources #1 and #2, respectively. The "×" marks in the figures indicate the true locations of the sources, which agree with two local maxima of P_{music}. The exact values of estimated locations with interpolation are listed as "Estimated " in Table 1. In this case we can estimate the locations and orientations with the small errors of several centimeters and several degrees, respectively.

3.2 Finite-size current loop sources

Next, we have a 70 cm×70 cm (the radius of its circumcircle is 50 cm) square loop source placed with its loop plane horizontally, at the frequency of 10 kHz with the SNR around 40 dB. We put five triaxial search coil sensors arranged in the vertical ($x-y$) plane at the locations (x, y, z) = (0, 0, 0), (1, 0, 0), (2, 0, 0), (1, 0, 1), (1, 0, -1) [m], at each of which the sensor measures the x-, y-, and z-components of the magnetic field. As mentioned in the previous section, first we try to estimate its center location and orientation by using the magnetic dipole model when scanning the MUSIC cost function P_{music}. Fig. 3 (a) shows the P_{music} distributions obtained with the magnetic dipole model over the $x-y$ (horizontal) plane at $z = -0.2$ m. The "×" mark and the square in the figure indicate the center location and outline of the current loop. The exact center location and the estimated location are listed as "True" and "Estimated (dipole)" in Table 2. In this case the center location of the square loop is surprisingly well estimated by the MUSIC dipole model with the estimation error almost the same as in the case of magnetic

dipole localization in 3.1. Then we estimate the size of the loop by re-scanning the P_{music} for various-size hexagonal loops put at the locations in the vicinity of the estimated dipole location. The solid line in Fig. 4 (b) shows the variation of P_{music} with various loop radius (circumcircles of the hexagonal loops) where the maximum value of P_{music} should indicate the estimated size of the current loop. In this case the estimated value of 0.45 m is in fairly good agreement with the true size of the square loop (circumcircle 50 cm). The estimated center location of the loop is indicated by the "○" mark in Fig. 4 (a). Fig. 4 (b) also plots the radius estimation for larger square loops with circumcircle radii of 70 cm and 100 cm, respectively, by the dashed and dotted lines. Shown as the "Estimated (loop)" radii in Table 2, they are estimated fairly well, with the error less than 10 cm.

We also try to estimate an "oblique" loop with the orientation of the loop normal pointing to the direction of (1, 1, 1), the center of which is placed at the same location as in the previous case. Fig. 4 (a) shows the P_{music} distribution with the dipole model, where the center of the 50 cm-loop looks almost accurately estimated. Fig. 4 (b) and Table 3 show the radius estimation for the oblique loops with the radii of 50 cm, 70 cm, and 100 cm. In this case the P_{muisic} maxima become not so well-defined and the estimated radii tend to be smaller than the true values. This would be caused by that we have fixed the orientations of the loops as those estimated with the dipole model.

5. Conclusion

We have extended the MUSIC algorithm to localize finite-size low-frequency current loops. We have confirmed the effectiveness of the algorithm to estimate the sizes as well as the locations and orientations of the finite-size current loop sources. This technique, however, would have larger estimation errors for the loop sources whose loop planes becoming more parallel to the sensor arrangement, for which we need to improve the localization accuracy in the future.

Acknowledgements

This work was mainly supported by Research Project "Control of Electromagnetics Environment in Low Frequency Band Less Than 100 kHz" of the Reclamation Research Promotion Business in the Future of Japan Society for the Promotion of Science (JSPS). Part of this work was also supported by the JSPS Grant-in-Aid for Scientific Research (Young Scientists (B), No. 14750287), and Takahashi Industrial and Economic Research Foundation.

References

[1] Ishibana, K., S. Yagitani, I. Nagano, M. Kawauchi, Y. Yoshimura, H. Hayakawa, and K. Tsuruda, "Localization and visualization of low-frequency electromagnetic sources," in *Proc.* EMC, Sendai, 2004.

[2] Mosher, J. C., P. S. Lewis, and R. M. Leahy, "Multiple dipole modeling and localization from spatio-temporal MEG data," *IEEE Trans. Biomedical Engineering*, vol. 39, no. 6, pp. 541–557, Jun. 1992.

[3] Audone, B., and M. B. Margari, "The use of MUSIC algorithm to characterize emissive sources," *IEEE Trans. Electromagnetic Compatibility*, vol. 43, no. 4, pp. 688–693, Nov. 2001.

[4] Schmidt, R. O., "Multiple emitter location and signal parameter estimation," *IEEE Trans. Antenna and Propagation*, vol. AP-34, no. 3, pp. 276–280, Mar. 1986.

[5] Schmidt, R. O., "Multilinear array manifold interpolation," *IEEE Trans. Antenna and Propagation*, vol. 40, no. 4, pp. 857–866, Apr. 1992.

Table 1: Source parameters for magnetic dipoles

	Location [m]	Orientation(d_x, d_y, d_z)
#1 : True	(1.72, 1.25, 0.14)	(0.71, 0.00, 0.71)
#1 : Estimated	(1.71, 1.28, 0.13)	(0.71, 0.01, 0.70)
#2 : True	(0.88, 0.96, -0.45)	(0.00, 0.00, 1.00)
#2 : Estimated	(0.88, 0.98, -0.45)	(-0.00, -0.01, 1.00)

Table 2: Source parameters for finite-size horizontal current loops

10.0 kHz	Location [m]	Orientaion (d_x, d_y, d_z)	Radius [cm]
True	(1.04, 1.26, -0.16)	(0.00, 0.00, 1.00)	50
Estimated (dipole)	(1.04, 1.19, -0.16)	(0.00, -0.01, 1.00)	—
Estimated (loop)	(1.04, 1.27, -0.15)	(0.00, -0.01, 1.00)	45
True	(1.04, 1.26, -0.16)	(0.00, 0.00, 1.00)	70
Estimated (dipole)	(1.03, 1.12, -0.14)	(0.00, -0.03, 1.00)	—
Estimated (loop)	(1.04, 1.28, -0.13)	(0.00, -0.03, 1.00)	60
True	(1.04, 1.26, -0.16)	(0.00, 0.00, 1.00)	100
Estimated (dipole)	(1.07, 1.04, -0.12)	(-0.00, -0.07, 1.00)	—
Estimated (loop)	(1.05, 1.35, -0.09)	(-0.00, -0.07, 1.00)	88

Table 3: Source parameters for finite-size oblique current loops

10.0 kHz	Location [m]	Orientaion (d_x, d_y, d_z)	Radius [cm]
True	(1.04, 1.26, -0.16)	(0.58, 0.58, 0.58)	50
Estimated (dipole)	(1.09, 1.26, -0.10)	(0.60, 0.54, 0.59)	—
Estimated (loop)	(1.08, 1.25, -0.12)	(0.60, 0.54, 0.59)	29
True	(1.04, 1.26, -0.16)	(0.58, 0.58, 0.58)	70
Estimated (dipole)	(1.14, 1.22, -0.05)	(0.61, 0.51, 0.61)	—
Estimated (loop)	(1.12, 1.25, -0.07)	(0.61, 0.51, 0.61)	42
True	(1.04, 1.26, -0.16)	(0.58, 0.58, 0.58)	100
Estimated (dipole)	(1.23, 1.22, 0.05)	(0.65, 0.45, 0.61)	—
Estimated (loop)	(1.16, 1.22, -0.00)	(0.65, 0.45, 0.61)	67

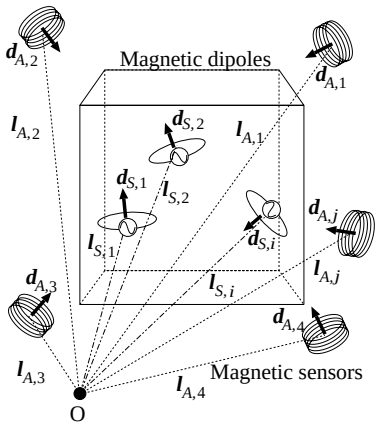

Figure 1: Magnetic dipole sources and magnetic sensors

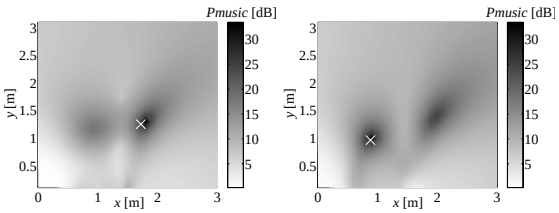

(a) $z = 0.0$ m (b) $z = -0.4$ m

Figure 2: Estimated source locations of two magnetic dipoles

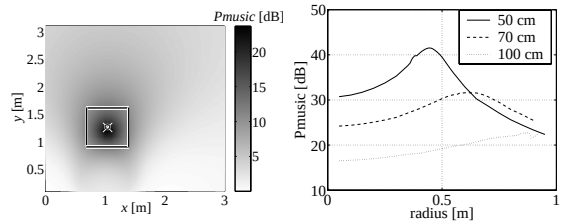

(a) $z = -0.2$ m (b)radius estimation

Figure 3: Estimatied source location and radius of a finite-size horizontal square loop

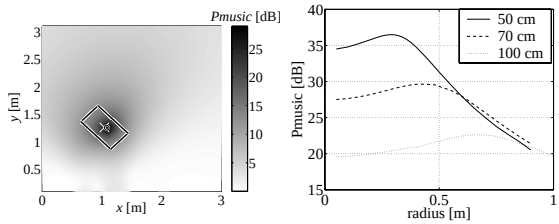

(a) $z = -0.1$ m (b)radius estimation

Figure 4: Estimatied source location and radius of a finite-size oblique square loop